BIOCHEMISTRY
including biophysical chemistry & molecular biology
Article

Biochemistry **2009,** *48,* 11971–11981 11971
DOI: 10.1021/bi901637c

Peptidomics of Prolyl Endopeptidase in the Central Nervous System[†]

Whitney M. Nolte,[‡] Debarati M. Tagore,[‡] William S. Lane,[§] and Alan Saghatelian*,[‡]

[‡]*Department of Chemistry and Chemical Biology, Harvard University, 12 Oxford Street, Cambridge, Massachusetts 02138, and* [§]*Mass Spectrometry and Proteomics Resource Laboratory, Center for Systems Biology, Harvard University, Cambridge, Massachusetts 02138*

Received September 18, 2009; Revised Manuscript Received November 9, 2009

ABSTRACT: Prolyl endopeptidase (Prep) is a member of the prolyl peptidase family and is of interest because of its unique biochemistry and connections to cognitive function. Using an unbiased mass spectrometry (MS)-based peptidomics platform, we identified Prep-regulated peptides in the central nervous system (CNS) of mice by measuring changes in the peptidome as a function of Prep activity. This approach was validated by the identification of known Prep substrates, such as the neuropeptide substance P and thymosin-β4, the precursor to the bioactive peptide Ac-SDKP. In addition to these known substrates, we also discovered that Prep regulates many additional peptides, including additional bioactive peptides and proline rich peptides (PRPs). Biochemical experiments confirmed that some of these Prep-regulated peptides are indeed substrates of the enzyme. Moreover, these experiments also supported the known preference of Prep for shorter peptides while revealing a previously unknown cleavage site specificity of Prep when processing certain multi-proline-containing peptides, including PRPs. The discovery of Prep-regulated peptides implicates Prep in new biological pathways and provides insights into the biochemistry of this enzyme.

Prolyl endopeptidase (Prep),[1] also commonly termed prolyl oligopeptidase (POP) (EC 3.4.21.26), was first identified as an oxytocin cleaving activity in the human uterus (*1*) and is part of the prolyl peptidase family of enzymes (*2*, *3*). Other mammalian members of the prolyl peptidase family include the dipeptidyl peptidases, such as the anti-diabetic target dipeptidyl peptidase 4 (DPP4) (*4*), and the recently characterized prolyl endopeptidase-like (PrepL) (*5*), which has been genetically linked to hypotonia-cystinuria syndrome (HCS) (*6*−*8*). Prep has been of general interest because of its unique biochemical activity as a proline endopeptidase. Unlike the cleavage activity of the dipeptidyl peptidases, which are restricted to N-terminal dipeptide cleavage (*3*, *9*), Prep proteolysis occurs at internal prolines in a peptide (*10*−*12*). On the basis of the known preference of Prep for cleavage at a proline, many proline-containing bioactive peptides have been tested, and identified, as Prep substrates in vitro (*12*). These substrates range from the tripeptide, thyrotropin-releasing hormone to a 31-amino acid peptide, β-endorphin (*2*, *13*).

A handful of the candidate neuropeptide substrates have been confirmed as physiological substrates of Prep through immunohistochemical or radioimmunoassay measurements of peptide levels in tissues where Prep activity has been pharmacologically inhibited (*14*−*17*). On the basis of the known bioactivities of physiological Prep substrates, new hypotheses regarding the biological function of Prep were developed and tested. For example, the Prep substrate vasopressin (*14*) has been linked to memory formation, which prompted tests of Prep inhibitors as anti-amnesic compounds (*18*). Interestingly, Prep inhibitors have shown improvements in memory and general cognitive function in rats (*18*, *19*), monkeys, and humans (*20*). Moreover, Prep has also been suggested to regulate the action of mood stabilizers such as lithium and valproate (*21*). However, many questions about the molecular mechanisms that connect Prep to these biological phenomena remain unanswered.

One major effort in trying to understand the cellular and physiological function of Prep has been the characterization of physiological substrates of the enzyme (*14*, *16*−*18*, *22*). In recent years, efforts to identify endogenous peptidase substrates have relied on the development and application of mass spectrometry (MS)-based peptidomics approaches (*23*, *24*) that identify changes in the peptidome associated with changes in the activity of a particular enzyme (*22*, *25*−*28*). For example, peptidomics has identified neuropeptides regulated by prohormone convertases (PCs) (*26*) and carboxypeptidase E (CPE) (*25*) in the nervous system, including a number of novel neuropeptides. In contrast to traditional antibody-based approaches, which are limited to a single peptide at a time (*14*, *16*−*18*, *22*), peptidomics approaches make unbiased measurements across the peptidome to enable the identification of enzyme-regulated peptides, including unknown peptides (*23*, *24*, *27*).

Recently, an isotope labeling peptidomics approach was applied to Prep in the nervous system of rats (*22*). These studies were able to identify modest changes in a number of peptides stemming from Prep inhibition, including some potentially novel substrates of the enzyme. Here, we build on these studies and apply our label-free peptidomics platform (*28*) to analyze changes

[†]This work was supported by National Institutes of Health Grant 1DP2OD002374 (A.S.), a Burroughs Wellcome Fund Career Award in the Biomedical Sciences (A.S.), a Searle Scholars Award (A.S.), and Training Grant T32GM07598 from the National Institutes of Health (W.M.N.).

*To whom correspondence should be addressed. Phone: (617) 384-8251. Fax: (617) 495-1792. E-mail: saghatelian@chemistry.harvard.edu.

[1]Abbreviations: ABPP, activity-based protein profiling; CD, circular dichroism; CGRP, calcitonin gene-related peptide; CNS, central nervous system; CPE, carboxypeptidase E; DPP4, dipeptidyl peptidase 4; HCS, hypotonia-cystinuria syndrome; LC, liquid chromatography; MALDI, matrix-assisted laser desorption ionization; MS, mass spectrometry; PC, prohormone convertases; PRD, proline rich domains; PRP, proline rich peptide; Prep, prolyl endopeptidase; PrepL, prolyl endopeptidase-like; PTM, post-translational modification; Z-Gly-Pro-AMC, *N*-carbobenzoxy-glycyl-prolyl-7-amido-4-methylcoumarin.

Published on Web 11/13/2009

associated with Prep inhibition in the CNS of mice. Our analysis revealed a number of Prep-regulated peptides, including novel substrates and products of the enzyme. Interestingly, there was no overlap in identified substrates with the previous study (*22*), which is likely due to differences in the inhibitor, animal model, and methodology. In general, our data provide insights into the pathways and biology that Prep might regulate in vivo through the identification of bioactive peptide substrates. The data also revealed an unappreciated class of Prep substrates that are fragments of proline rich domains (PRDs), which are typically termed proline rich peptides (PRPs) (*29*). Biochemical studies confirmed some of the Prep-regulated peptides as substrates. This work also revealed that Prep can selectively cleave after individual prolines in multi-proline-containing peptides. Together, these studies demonstrate the value of peptidomics in gaining insight into the biology and biochemistry of Prep through the discovery and analysis of natural substrates.

EXPERIMENTAL PROCEDURES

Reagents. S17092 was synthesized as previously described (*30*). Mouse CGRP(1−37) was purchased from American Peptide Company, Inc. (Sunnyvale, CA).

Animal Studies. Wild-type (WT) mice (C57BL/6) used in this study were either purchased (Jackson Laboratories, Bar Harbor, ME) or taken from a breeding colony. Animals were kept on a 12 h light−12 h dark schedule and fed ad libitum. For pharmacological studies, S17092 (30 mg/kg in 10% Tween 80 in water) or vehicle (10% Tween 80 in water) was injected (intraperitoneally), and mice were sacrificed 1 or 4 h later. For tissue collection, animals were euthanized with CO_2, and their tissues were dissected, flash-frozen with liquid nitrogen, and stored at −80 °C. All animal care and use procedures were in strict accordance with the standing committee on the use of animals in research and teaching at Harvard University and the National Institutes of Health guidelines for the humane treatment of laboratory animals.

Isolation of Physiological Peptides from Tissue. Frozen tissues, stored at −80 °C, were boiled in 200−300 μL of boiling water for 10 min to denature any enzymes and eliminate proteolytic activity prior to homogenization. The aqueous fraction was collected and saved, and the tissue was dounce-homogenized in 0.25% ice-cold acetic acid. The aqueous fraction and the homogenate were combined and centrifuged at 20000*g* for 20 min at 4 °C. The supernatant was then sent through a 10 kDa molecular mass cutoff filter (Microcon YM-10, Millipore), and the filtrate containing the peptides was concentrated in a speed vacuum concentrator and resuspended in 0.1% formic acid prior to analysis by LC−MS.

LC−MS/MS Experiments. Aliquots (2−10 μL) were injected onto a Waters nanoAcquity HPLC system configured with in-house packed 75 μm reverse-phase capillary trapping and analytical columns (New Objective, Woburn, MA) coupled to an LTQ-Orbitrap mass spectrometer (ThermoFisher Scientific, San Jose, CA). The liquid chromatography gradient proceeded from 3 to 33% acetonitrile in water (0.1% formic acid) over 180 min. Mass spectra from m/z 395 to 1600 were acquired in the Orbitrap instrument with a resolution of 60000, while the six most abundant ions were targeted for concurrent MS/MS in the linear ion trap with a relative collision energy of 30%, 2.5 Da isolation width, and recurring ions dynamically excluded for 60 s. Sequencing was facilitated by the SEQUEST algorithm with differential modification of methionine to its sulfoxide, C-terminal amidation, acetylation, and phosphorylation. The mouse subset of the UniprotKB FASTA database (MGI, ftp://ftp.informatics.jax.org/pub/sequencedbs/seq_dbs.current/uniprotmus.Z) concatenated to a reversed decoy database was used for peptide identification and served to estimate a false discovery rate (FDR). Peptides were accepted within 3 ppm of the expected mass meeting a series of custom filters on ScoreFinal (Sf), −10 Log P, and charge state that attained an average peptide FDR of $<2\%$ across data sets. Manual inspection of spectra, FDR calculation, and protein inference were performed in a customized version of Proteomics Browser Suite 2.23 (Thermo Fisher Scientific).

Data Analysis. Differences in the peptide pool were identified using XCMS, which uses nonlinear retention time alignment and peak areas to quantify changes between sample sets. Peptides specifically associated with one treatment class were confirmed by integration of the peaks in the extracted ion chromatograms, and these areas were used to quantify the relative differences of a peptide between genotypes. A Student's t test was used to assess the statistical significance of these differences.

Recombinant Prep Expression. A plasmid containing the mouse Prep gene was purchased (Open Biosystems), and the coding sequence was subcloned between the XhoI and EcoRI sites of a pTrcHisA vector (Invitrogen). The final pTrcHisA-wtPrep construct contains an N-terminal His6 tag fused to the coding sequence of Prep. The pTrcHisA-PrepD35A-K196A plasmid was constructed using the pTrcHisA-Prep construct and a QuikChange site-directed mutagenesis kit (Stratagene, La Jolla, CA). Rosetta2(DE3)pLysS (Stratagene) cells transformed with pTrcHisa-wtPrep or pTrcHisa-PrepD35A-K196A were grown at 37 °C in Luria broth containing 100 μg/mL ampicillin and 34 μg/mL chloramphenicol, and expression was induced by the addition of IPTG to a final concentration of 1 mM when the OD_{600} of the culture reached 0.4−0.5. Induced cultures were grown overnight at 18 °C for wild-type Prep and 30 °C for the double mutant (pTrcHisa-PrepD35A-K196A). Recombinant proteins were purified by Ni(II) affinity chromatography. Further purification was performed using a Superdex 200 10/300 column (GE Healthcare) with a mobile phase of 50 mM phosphate buffer and 0.15 M NaCl (pH 7.0).

Peptide Synthesis and Purification. Peptide substrates were synthesized manually using solid-phase peptide synthesis or purchased from Biomatik Corp. (Wilmington, DE). Crude peptides were purified by RP-HPLC (Shimadzu) using a C18 column (150 mm × 20 mm, 10 μm particle size, Higgins Analytical). The HPLC gradient varied depending on the peptide (mobile phase A consisted of 99% H_2O, 1% acetonitrile, and 0.1% TFA; mobile phase B consisted of 90% acetonitrile, 10% H_2O, and 0.07% TFA). HPLC fractions were analyzed by MALDI-TOF (Waters) to confirm the correct sequence of the peptide using α-cyano-4-hydroxycinnamic acid as the matrix, and the pure fractions were combined and lyophilized.

In Vitro Mass Spectrometry Assays of Peptide Processing. Peptides (100 μM) were added to recombinant Prep (30−300 nM) and incubated at 37 °C for 1 h in 25 mM sodium phosphate with 0.5 mM EDTA and 2 mM DTT (pH 7.0). The reactions were quenched with 8 M guanidinium-HCl and then desalted using Zip-Tips (C18, Millipore). MALDI-TOF was performed with α-cyano-4-hydroxycinnamic acid as the matrix. Reaction products were also observed using LC−MS. MALDI samples were diluted 10-fold into 0.1% formic acid in water.

Aliquots (5−10 μL) were injected onto an Eksigent nanoLC-2D HPLC system configured with a prepacked IntegraFrit trapping column (ProteoPep II C18, 300 Å, 5 μm) and an in-house packed reverse-phase picotip analytical column (New Objective) coupled to an LTQ mass spectrometer (ThermoFisher Scientific). The liquid chromatography gradient proceeded from 5 to 65% acetonitrile in water (0.1% formic acid) over 40 min. Mass spectra were acquired from *m*/*z* 400 to 2000 followed by targeting the three most abundant ions for MS/MS.

Circular Dichroism. CGRP(1−37), CGRP(20−37), and dsCGRP(1−37) were dissolved in 50 mM Tris-HCl with 1 mM EDTA (pH 7.5) at a concentration of 100 μM. All other peptides were dissolved in 25 mM sodium phosphate with 0.5 mM EDTA and 2 mM DTT (pH 7.0) at concentrations of 100−500 μM. CD spectra were recorded on a Jasco J-710 spectropolarimeter at 20 °C using the following standard measurement parameters: wavelength, 190−260 nm; step resolution, 0.5 nm; speed, 100 nm/s; number of accumulations, 4; response, 1 s; bandwidth, 1 nm; path length, 0.1 cm.

In Vitro Kinetic Assays. The kinetics experiments were performed using an LC−MS-based assay. The concentrations of the peptide stocks were determined by amino acid analysis (Commonwealth Biotechnologies Inc., Richmond, VA). Peptides (0.5−100 μM) were incubated with recombinant Prep (5−100 nM) in 50 mM Tris-HCl with 1 mM EDTA (pH 7.5) at 25 °C for 5−60 min. The time and concentration of the enzyme were varied to ensure less than 20% conversion of substrate so that the reaction rate remained linear. After the reaction had been quenched with TFA (final concentration of 10%), analysis was performed by direct injection of the samples onto a LC−MS-TOF spectrometer (Agilent ESI-TOF, Agilent Technologies) fitted with a Gemini C18 column (50 mm × 4.6 mm, 5 μm particle size, Phenomenex) using a binary gradient (A consisted of H_2O and 0.1% formic acid, and B consisted of ACN and 0.1% formic acid) from 10 to 50% B over 15 min. The peak areas served to quantify the different peptides generated during the incubation with Prep, and standard curves of the product were used to determine the absolute concentration of the peptides generated in the reaction. The kinetics data were fitted to the Michaelis−Menten equation using KaleidaGraph (Synergy software). Each determination of the parameters was obtained from at least three replicates.

Prep Inhibition with CGRP(1−37). The kinetics experiments were performed using an LC−MS-based assay. Substance P (100 μM) was incubated with 10 nM recombinant Prep in the presence of varying concentrations of CGRP(1−37) (from 10 nM to 200 μM) in 50 mM Tris-HCl with 1 mM EDTA at 25 °C for 60 min. After the reaction had been quenched with TFA (final concentration of 10%), product formation was assessed by direct injection of the samples onto a LC−MS-TOF spectrometer (Agilent ESI-TOF, Agilent Technologies) as described for the in vitro kinetic assays. The peak areas served to quantify the product generated during the incubation. The inhibition data were fitted to a dose−response logistic equation using KaleidaGraph (Synergy software). The data shown are the result of three replicates.

Prep Lysate Activity Assays. C57BL/6 mice were sacrificed and the spinal cords collected and stored at −80 °C prior to use. To test the effect of boiling on Prep activity, one spinal cord from a mouse was dounce-homogenized in 400 μL of ice-cold assay buffer [25 mM sodium phosphate, 0.5 mM EDTA, and 2 mM DTT (pH 7.0)], while the other spinal cord was heated in boiling water for 10 min prior to homogenization in assay buffer. Following centrifugation at 20000*g* for 20 min at 4 °C, Prep activity was measured in the lysate using the fluorogenic substrate Z-Gly-Pro-AMC (Bachem, Inc.). The assay was performed by addition of Z-Gly-Pro-AMC in assay buffer (final concentration of 20 μM) to 100 μL of lysate (0.5 mg/mL) in both the absence and presence of 2 μM S17092. The fluorescence was monitored at 37 °C using an excitation wavelength of 360 nm and an emission wavelength of 460 nm (Spectramax Gemini XS plate reader, Molecular Devices).

Transfection of COS-7 Cells with Prolyl Peptidases and Lysate Preparation. COS-7 cells were maintained in DMEM supplemented with FBS, penicillin, and streptomycin. Clones of members of the prolyl peptidase family (Prep, Prepl, DPP4, DPP7, DPP8, DPP9, and FAP) were obtained from Open Biosystems in PCMV or PCMVsport vectors and used directly or subcloned into pcDNA3.1 for mammalian cell expression. Transfection of COS-7 cells with the indicated vectors was performed using Lipofectamine (Invitrogen) according to the manufacturer's instructions. Two days after transfection, the cells were washed with and resuspended in phosphate-buffered saline (PBS). Cells were lysed by sonication. Soluble and membrane fractions were separated by ultracentrifugation at 100000*g*. The supernatant was kept as the soluble fraction, and the pellet was resuspended in 100 μL of PBS. All lysates were diluted to 1 mg/mL. Protein concentrations were determined by the Bradford assay.

S17092 Specificity by Competitive ABPP (31). COS-7 cell lysates with overexpressed members of the prolyl peptidase family (Prep, Prepl, DPP4, DPP7, DPP8, DPP9, and FAP) were used to screen the selectivity of S17092. COS-7 cell lysates at 1 mg/mL were incubated with 2 μM S17092 or vehicle (PBS with a final DMSO concentration of 1%) for 10 min at room temperature. The lysates were then incubated with 2 μM FP-rhodamine (*32*) for 30 min. Reactions were quenched with SDS−PAGE loading buffer (reducing), and mixtures were separated by SDS−PAGE (10% acrylamide) and visualized in-gel with a GE Typhoon flatbed fluorescence scanner. The selectivity of S17092 was also tested in spinal cord lysates. Mouse spinal cords were homogenized in PBS. The lysates were centrifuged at 5000*g* to remove debris, and protein concentrations were determined with a Bradford assay. The ABPP assay was performed on 1 mg/mL spinal cord lysates exactly as for COS-7 lysates (see above).

RESULTS

Determining the Selectivity of S17092 for Prep. We set out to identify Prep substrates by measuring changes in the peptidome as a function of Prep inhibition, which was accomplished using a pharmacological inhibitor, S17092 (*30*) (Figure 1). As a Prep inhibitor, S17092 has been shown to be potent and specific in vitro and in vivo (*17*, *33*). However, since the development of S17092 the number of prolyl peptidases has grown, including the recent discovery of prolyl endopeptidase like PrepL (*5*−*7*), which is most homologous to Prep of all the members of the prolyl peptidase family (*3*). Despite this similarity, to the best of our knowledge, S17092 has never been tested for its selective inhibition of Prep over PrepL, which is an important factor in our experiments.

Each of the prolyl peptidases was overexpressed in COS-7 cells, and cell lysates containing the different prolyl peptidases were used in a competitive activity-based protein profiling

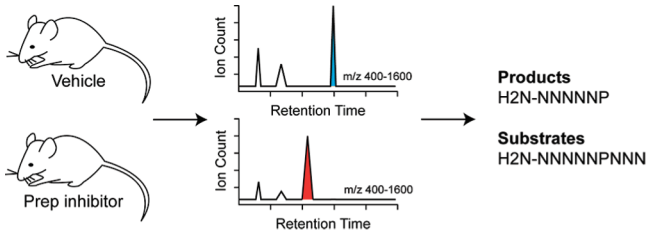

FIGURE 1: Workflow for peptidomics analysis of Prep-regulated peptides. Peptides are isolated from mice treated with vehicle or the Prep inhibitor, S17092. LC−MS analysis of the peptidome is followed by data analysis with XCMS, which quantifies changing ions between two treatment conditions. The peptide sequences of these ions are then determined using tandem MS spectra and SEQUEST. These ions often consist of substrates or products of the peptidase.

(ABPP) assay (*31*) to assess the selectivity of S17092. Competitive ABPP measures the labeling of serine hydrolases with a fluorescent activity-based probe, FP-rhodamine (*32*), in the presence and absence of an inhibitor. If the inhibitor binds to the enzyme, the labeling is blocked and the subsequent fluorescent signal of the labeled protein on an SDS−PAGE gel is diminished in magnitude or absent (*31*). Using this assay, we were able to demonstrate that S17092 does not inhibit any of the dipeptidyl peptidases (DPP4, -7, -8, and -9 and fibroblast activation protein) or PrepL (Figure 2A and the Supporting Information), confirming its specificity as a Prep inhibitor. The selectivity of S17092 for Prep was further demonstrated by a competitive ABPP assay in spinal cord lysates. Only the band corresponding to Prep disappeared upon S17092 addition, indicating that, of the serine hydrolases labeled by the ABPP reagent, only Prep is inhibited by S17092 (Figure 2B).

Peptidomics Experiments Using Prep Selective Inhibitor S17092. The workflow for our peptidomics experiments consists of four key steps: isolation of the peptide from tissues of S17092 and vehicle-treated mice, LC−MS analysis, XCMS processing to discover changes in ion abundance between two samples (*34*), and, finally, identification of the peptides using SEQUEST (*35*) (Figure 1). Mice were treated with S17092 (30 mg/kg) via an intraperitoneal injection. Inhibition of Prep was assessed by comparing S17092-treated tissue lysates to those from vehicle-treated mice for residual Prep activity using a selective fluorescent Prep substrate, Z-Gly-Pro-AMC (*36*). In initial experiments, mice were treated with S17092 for 4 h prior to tissue isolation. We found approximately 8% activity in tissues from S17092 mice when compared to vehicle-treated mice (Figure 2C), indicating that S17092 was able to be distributed into the nervous system and inhibit the enzyme.

For our peptidomics experiments, the relevant tissue is isolated and processed to maximize the integrity of the peptidome. Specifically, the tissue is heated prior to tissue homogenization as a means of eliminating any enzymatic activity, especially proteolytic activity, which might degrade our peptides or generate additional peptides through the proteolysis of proteins (*23*, *27*, *37*). We confirmed the effectiveness of this heat denaturation step by the absence of Prep activity in heat-treated samples (Supporting Information). After being heated, tissue samples were homogenized, and endogenous peptides were separated from larger proteins by filtration through a molecular mass cutoff filter (10 kDa). This filtrate was then concentrated and analyzed by LC−MS.

Differences in the peptidome were identified by comparison of the LC−MS data sets from S17092-treated samples to vehicle-treated samples using XCMS. XCMS is a comparative profiling

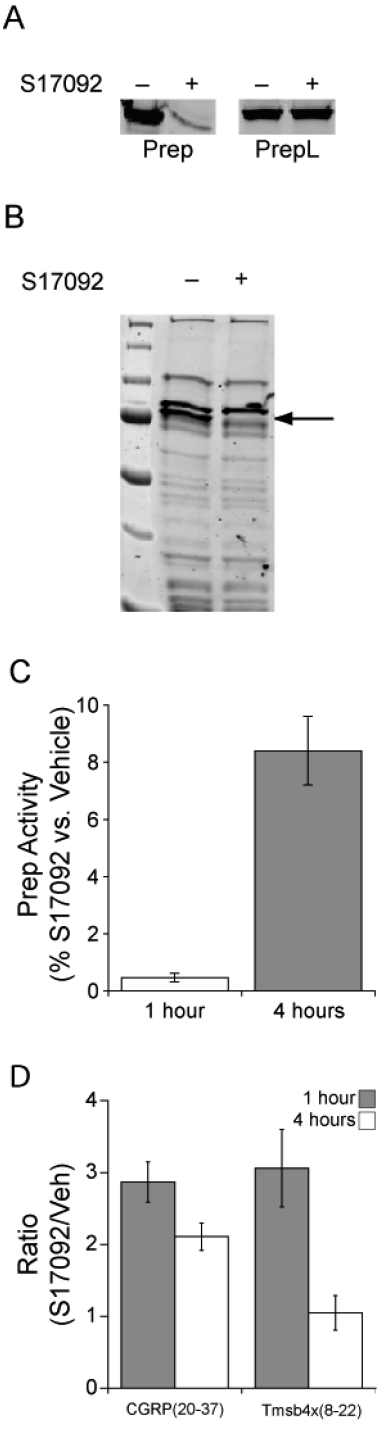

FIGURE 2: S17092 selectivity and optimal conditions for peptidomics. (A) S17092 was screened against Prep and PrepL using a competitive ABPP assay with FP-rhodamine as the probe. S17092 (2 μM) selectively inhibits labeling of Prep (left) but does not alter PrepL labeling (right) in lysates (1 mg/mL) of transfected COS-7 cells. (B) S17092 selectively inhibits Prep in spinal cord lysates. S17092 (2 μM) or vehicle was added to spinal cord lysates (1 mg/mL) in a competitive ABPP assay with FP-rhodamine as the probe. The arrow indicates the Prep band that is the only band that disappears upon addition of S17092. (C) Prep activity in spinal cord lysates 1 and 4 h post-intraperitoneal injection of S17092 (30 mg/kg) using a selective Prep substrate, Z-Gly-Pro-AMC. The activity is represented as a percentage of the residual activity in the S17092-treated sample when compared to the vehicle-treated sample. (D) Levels of Prep substrates in the spinal cord 1 and 4 h after intraperitoneal S17092 administration. The level of CGRP(20−37) is significantly elevated at 1 h (gray bar) and 4 h (white bars), while the level of Tmsb4(8−22) is elevated only at 1 h.

Table 1: Relative Levels of Peptides Measured by Peptidomics in the Central Nervous System (CNS) of Mice Treated with the Prep Inhibitor S17092 or Vehicle

sequence[a]	precursor protein (peptide region)	S17092/vehicle[a]
	Vehicle-Elevated Peptides	
Ac-MNTSFTRKSH[c]	2′,3′-cyclic-nucleotide 3′-phosphodiesterase, Cnp(1−10)	0.43[b]
NVGSEAF-NH_2[a]	calcitonin gene-related peptide 1, CGRP(31−37)	0.53[c]
Ac-ADKEAGGGDAGPRETAP[a]	heat shock protein 12A, Hsp12a(2−18)	0.12[b]
KGPGPGGPGGAGGARGGAGGGP[c]	neurogranin, Nrgn(54−75)	0.15[b]
EEEANGGEILA[a]	preproenkephalin 1, Penk(123−133)	0.20[c]
GRGS(Phos)EEDRAP[a,c]	chromogranin B precursor, Chgb(362−371)	0.10[ac]
LLEAAQEEGAVTPDLPGLEKVQVRP[a]	thyroliberin precursor, Trh(25−49)	0.26[c]
APPEPVPPPRAAP[a,b]	VGF nerve growth factor, Vgf(490−502)	0.24[ab]
	S17092-Elevated Peptides	
GGVVKDNFVPTNVGSEAF-NH_2[a]	calcitonin gene-related peptide I, CGRP(20−37)	2.9[c]
EPPPPEPPRI[a,b]	Cd99 antigen-like 2, Cd99l2(207−216)	3.5[bb]
APPGVPRITISDP[a,b]	dynamin 1, isoform 3 or 5, Dnm1(839−851)	3.9[c]
Ac-GPGPAPRK[a]	RIKEN cDNA 6330403L08, 6330403L08(222−229)	5.8[c]
PSPKTPPGSGEPPKS[c]	microtubule-associated protein tau, Mapt(485−499)	4.5[b]
MDELYPMEPEEEANGGEILA[a]	preproenkephalin 1, Penk(114−133)	3.0[b]
SAASAPLVETSTPLRL[a,b]	proSAAS precursor, Pcsk1n(44−59)	3.6[ac]
APLVETSTPLRL[b]	proSAAS precursor, Pcsk1n(48−59)	2.1[c]
RPKPQQFFGLM-NH_2[b]	substance P, Subp(1−11)	1.9[c]
LPEPAPPRPS[b]	synapsin-1, Syn(673−682)	5.9[c]
SPPFTETLDTSSKGYQVPAY[b]	synaptogyrin-3, Sng3(210−229)	2.5[c]
Ac-SDKPDMAEIEKFDKS[a,b]	thymosin β4, Tmsb4x(8−22)	3.0[ac]
Ac-SDKPDMAEIEKFDKSKLK[b]	thymosin β4, Tmsb4x(8−25)	3.0[c]
APPGRPDVFPPPLSSE[a,b]	VGF nerve growth factor, Vgf(24−39)	3.3[ac]
APPEPVPPPRAAPAPTHV[a,b]	VGF nerve growth factor, Vgf(490−507)	3.7[bc]
	Unaffected Proline-Containing Peptides	
RPTLNELGISTPEELGLDKV[a]	cytochrome *c* oxidase subunit 5A, Cox5a(127−146)	1.1
TPRTPPPSQ[a]	mylein basic protein, Mbp(252−260)	1.7

[a] a, spinal cord; b, brain; c, hypothalamus. [b] $p \leq 0.05$. [c] $p \leq 0.01$.

software used to align, quantify, and statistically rank ions between two data sets (*34*), in this case S17092 and vehicle. To date, XCMS has primarily been used to analyze data from metabolomics experiments (*38*, *39*), but we were able to successfully apply this program to detect statistically significant changes in our S17092−vehicle data sets. Each of these changing ions identified by XCMS was manually validated by inspection and integration of the peaks in the extracted ion chromatograms, and these numbers were used to calculate all ratios. Finally, the sequences of these peptides are identified using their tandem MS (MS2) spectra and SEQUEST (*35*). During this analysis, we also searched for peptides with post-translational modifications, including acetylation, phosphorylation, and C-terminal amidation, which was important since many Prep-regulated peptides are modified (~40% of the final list of peptides).

Duration of S17092 Inhibition on a Number of Prep-Regulated Peptides. In initial experiments, only three peptides were identified as changing more than 2-fold in the spinal cords of mice treated with S17092 for 4 h. Previous work with S17092 revealed increased substance P brain levels when measured at earlier time points (1 h) after administration of S17092, but these levels returned back to baseline levels after chronic inhibition (*17*). The exact cause of this difference is unknown, but it prompted us to look at earlier time points in the spinal cord to account for possible compensatory mechanisms or the return of Prep activity. Either of these mechanisms could mask Prep-regulated peptides in the peptidome. Shifting our analysis point from 4 h to the 1 h time point identified significant changes in the same three peptides we initially measured at 4 hs, most with a greater change at 1 h (Supporting Information and Figure 2D). The analysis also revealed 12 additional peptides that were significantly changing only at the 1 h time point (Figure 2D and Table 1). Analysis of Prep activity at 1 and 4 h reveals substantially more activity at 4 h, which might explain the smaller number of changes at 4 h (Figure 2C).

On the basis of these results, subsequent profiling in the brain and hypothalamus was conducted following a 1 h treatment with S17092. Altogether, we identified 23 distinct peptides changing in response to Prep inhibition, with a large degree of overlap among the spinal cord, brain, and hypothalamus (Table 1). Importantly, we were able to detect changes in brain substance P levels, a known Prep substrate (*14*, *17*), which validated our peptidomics approach. Moreover, all of the peptides elevated in the Prep-inhibited samples contained a proline residue indicating that they are potential Prep substrates, and many of the peptides with elevated levels in the vehicle sample had a C-terminal proline, indicative of a Prep cleavage product. Importantly, not all proline-containing peptides are significantly changing in vivo. Next, we wanted to confirm that some of these peptides are bona fide substrates of Prep. Overall, the S17092 elevated peptides are longer and contain more prolines than typical Prep substrates (*2*, *12*). We selected a longer peptide with a single proline, CGRP(20−37), and a number of peptides with multiple prolines as substrates to test with Prep. These substrates are representative of the endogenous substrate pool and would provide a better understanding of the relationship between Prep and natural substrates.

A

GGVVKDNFVPTNVGSEAF-NH_2
aCGRP(20-37) **[CGRP(20-37)]**

S–S
SCNTATCVTHRLAGLLSRSGGVVKDNFVPTNVGSEAF-NH_2
aCGRP(1-37) **[CGRP(1-37)]**

SSNTATSVTHRLAGLLSRSGGVVKDNFVPTNVGSEAF-NH_2
diserine aCGRP(1-37) **[dsCGRP(1-37)]**

TNVGSEAF-NH_2
aCGRP(30-37) **[CGRP(30-37)]**

B

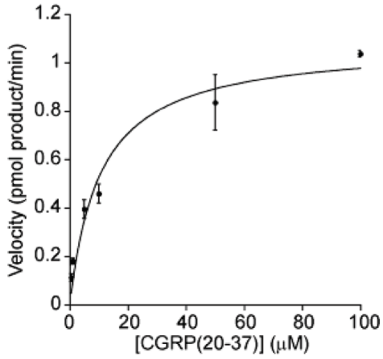

C

	Km (μM)	k_{cat} (s-1)	k_{cat}/km (M-1*s-1)	Relative rate vs. CGRP(20-37)
wtPrep				
CGRP(20-37)	10.5 ± 3	0.072 ± 0.006	$6.9x10^3$	1
dsCGRP(1-37)	12.5 ± 5	0.0020 ± 0.0002	$1.6x10^2$	0.02
CGRP(1-37)	4.3 ± 0.7	0.0012 ± 0.00005	$2.8x10^2$	0.04
PrepD35A-K196A				
CGRP(20-37)	1.2 ± 0.3	0.0051 ± 0.0003	$4.3x10^3$	1
dsCGRP(1-37)	3.4 ± 1	0.0023 ± 0.0002	$6.6x10^2$	0.15
CGRP(1-37)	-	-	$2.2x10^2$	0.05

D

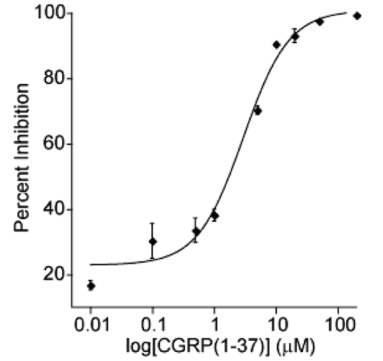

FIGURE 3: Experiments with CGRP peptides. (A) Sequences and nomenclature of CGRP peptides used throughout this work. (B) Rate vs substrate concentration plot for CGRP(20−37) with Prep indicating a single cleavage site enzyme−substrate reaction. (C) Kinetic parameters for the different substrates [CGRP(20−37), CGRP(1−37), and dsCGRP(1−37)] with wild-type Prep and PrepD35A-K196A show the strong preference of the enzyme for the shorter CGRP(20−37) peptide. Data represent averages ± standard errors (SE). (D) The inhibition of substance P (100 μM) degradation by Prep (10 nM) was monitored at varying concentrations of CGRP(1−37) (from 10 nM to 50 μM). CGRP(1−37) inhibited Prep activity with an IC_{50} of 2 μM.

Kinetic Studies with CGRP, CGRP Fragments, and CGRP Analogues. Prep is known to prefer shorter peptide substrates (*2*, *11*, *40*, *41*), and kinetic studies with peptides as long as 17 amino acids support this idea (*41*). However, a number of the peptides identified as Prep substrates through peptidomics are longer than the typically studied Prep substrates. We used the CGRP(20−37) substrate to verify that some of the longer peptides we identified can be cleaved by Prep. In addition, CGRP(20−37) was compared to full-length CGRP(1−37), which was unchanged in our peptidomics data (Supporting Information), to test whether the known preference of Prep for shorter peptides still applied for peptides as long as 18 amino acids, like CGRP(20−37). Since the Prep cleavage site in CGRP-(20−37), an endogenous substrate, and CGRP(1−37) are the same, any differences in catalysis should be due to differences in peptide structure or interactions between the protein and peptide at sites outside the cleavage site. In addition to these two CGRP peptides, a diserine mutant of CGRP(1−37), which we termed dsCGRP(1−37), was also analyzed and served as a control for secondary structure imposed by the internal disulfide bond found in the CGRP(1−37) structure (Figure 3). All three CGRP analogues have the same product peptide, CGRP(30−37). Kinetic measurements of the product peptide were performed by LC−MS.

First, these kinetics experiments confirmed that CGRP-(20−37) is a Prep substrate with a k_{cat}/K_m of 6.9×10^3 M^{-1} s^{-1}, supporting the notion that this peptide is an endogenous Prep substrate (Figure 3). In addition, comparison of CGRP-(20−37) to the full-length CGRP peptides, CGRP(1−37) and dsCGRP(1−37), demonstrated that Prep is sensitive to peptide length in agreement with previous reports (*11*, *42*). Specifically, the k_{cat}/K_m for CGRP(20−37) is 20-fold better than the activity toward CGRP(1−37) and 40-fold better than that toward dsCGRP(1−37) (Figure 3). These differences did not seem to be structural, as circular dichroism (CD) experiments showed that these peptides are mostly unstructured (Supporting Information), and little difference was observed in k_{cat}/K_m between CGRP(1−37) and dsCGRP(1−37). We also tested a mutant of Prep, PrepD35A-K196A, that lacks a key salt bridge, from D35 to K196, connecting the two domains found in Prep and lies in front of the active site (*40*, *43*). This mutant enzyme had a relaxed preference for shorter peptides as the k_{cat}/K_m value for dsCGRP-(1−37) was only 6-fold worse than that of CGRP(20−37) (Figure 3).

Interestingly, with PrepD35A-K196A, CGRP(1−37) deviated from hyperbolic kinetics (Supporting Information), most likely due to product inhibition at higher substrate concentrations, and we accounted for this by calculating k_{cat}/K_m as a second-order rate constant at lower concentrations. If all the substrates' k_{cat}/K_m values are calculated as second-order rate constants, the result is the same; PrepD35A-K196A has reduced specificity for shorter peptides (Supporting Information). These kinetic experiments with Prep and PrepD35A-K196A support previous studies that indicate that access to the Prep active site restricts cleavage to shorter peptides and defines a specific case, CGRP, in which this biochemical property of Prep enables this enzyme to regulate the CGRP(20−37) fragment without affecting the levels of bioactive CGRP(1−37) in vivo (Supporting Information).

CGRP Inhibition of Prep Activity. Since CGRP is such a poor substrate for Prep but still seems to bind to the enzyme, we

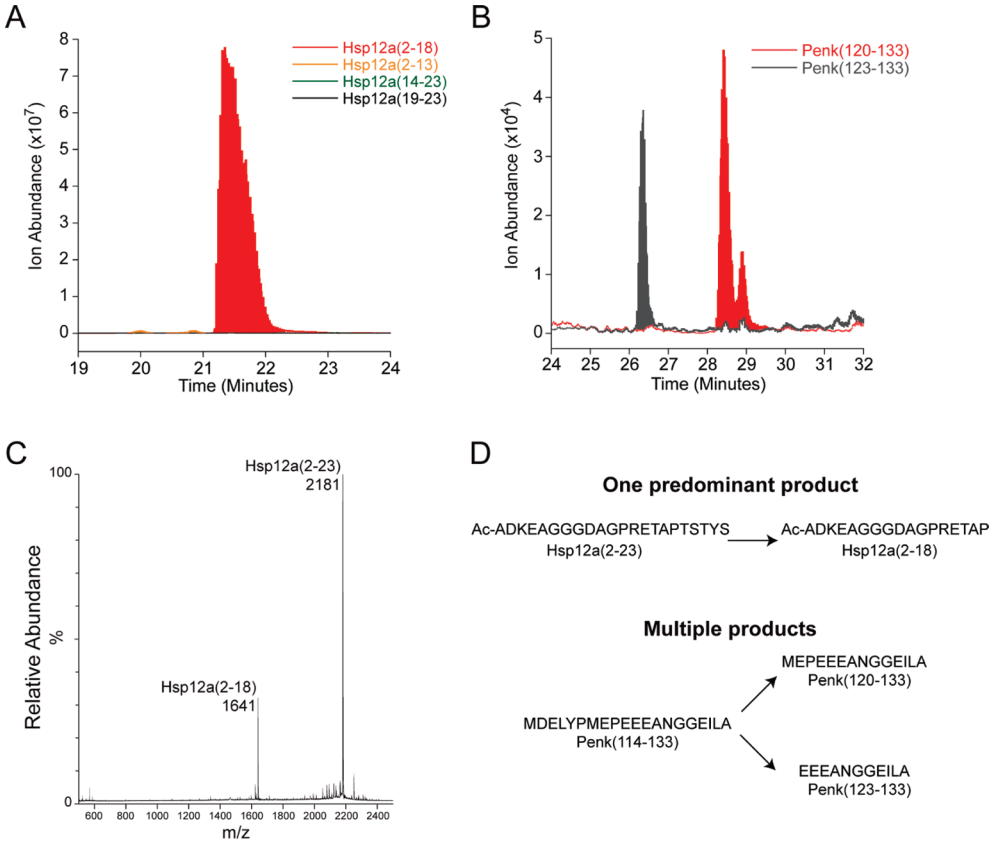

FIGURE 4: Prep cleavage of peptides with two proline residues. (A) LC−MS trace of Prep cleavage of Hsp12a(2−23) showing a single major product, Hsp12a(2−18). (B) Penk(114−133) processed to a similar extent at two positions, 120 and 123. (C) MALDI-MS spectrum of Hsp12a(2−23) that corroborates the LC−MS data and shows only a single predominant product, Hsp12a(2−18). (D) Cleavage pathways that generate the product distributions seen for Hsp12a(2−23) and Penk(114−133).

tested whether CGRP could inhibit Prep-mediated substance P catabolism. This stemmed from previous observations that increasing concentrations of CGRP weakened substance P degradation, enhancing and prolonging the effects of substance P (*44*, *45*), but the enzyme was never identified. In vitro cleavage assays with 100 μM substance P and 10 nM Prep in the presence of varying concentrations of CGRP indicated that CGRP inhibited the degradation of substance P with an IC_{50} of 2 μM.

In Vitro Experiments with Multi-Proline-Containing Substrates and Recombinant Prep. Interestingly, many of the Prep substrates we identified had two or more potential Prep cleavage sites denoted by prolines in their sequence. For example, the Penk(114−139) substrate contains two proline residues, while Cd99l2(207−216) has six prolines among its 10 amino acids (60%). Many of the peptides with more than two prolines come from a proline rich domain (PRD) of the full-length protein precursor, and we refer to any peptide with three or more prolines as a proline rich peptide (PRP).

These multi-proline substrates differ dramatically from known Prep substrates, which usually have a single proline, making it difficult to predict how these peptides would be processed. On the basis of the reported substrate selectivity of Prep, one would expect cleavage of the endogenous multi-proline substrates, including PRPs, at nearly every proline residue, except, perhaps, for proline repeats with three or more prolines (*46*). However, Prep-regulated peptides elevated in the vehicle samples still have intact prolines, even though the peptide appears to have been cleaved by Prep, suggesting that Prep might show some specificity between different prolines. This observation prompted us to test whether certain substrates, containing either two prolines or many prolines (e.g., PRPs), are preferentially cleaved by Prep at a single proline residue.

We began these studies by looking at peptides with two noncontiguous proline residues, Penk(114−133) and Ac-Hsp12a(2−23). The Ac-Hsp12a(2−18) peptide, a putative Prep product with an elevated level in the vehicle-treated sample, contained two prolines, one internal (position 13) and one at the C-terminus. This observation suggests that Prep cleaved this substrate at only one of two potential cleavage sites to produce the observed product. To test this, we added the next five amino acids in the Hsp12a sequence to Ac-Hsp12a(2−18) to generate the Ac-Hsp12a(2−23) peptide, a model substrate that we could use to assess Prep specificity. Analysis of the processing of the Penk(114−133) and Ac-Hsp12a(2−23) by Prep revealed that Penk(114−133) is cleaved at both prolines to approximately the same extent, while Ac-Hsp12a(2−23) is preferentially hydrolyzed at proline 18 (Figure 4). To ensure that this difference was not due in some way to the N-terminal acetyl group of the Hsp12a peptide, we tested an Hsp12a variant lacking the N-terminal acetyl group and found the same result (Supporting Information).

Next, we looked at two PRPs derived from the VGF nerve growth factor, Vgf(24−39) and Vgf(490−507). On the basis of the known selectivity of Prep, we would predict that both these peptides would be cut at multiple sites except for the tri-proline repeat, PPP (*46*), while our peptidomics data indicate that Vgf(490−507) might be predominantly cleaved at a single proline. Prep processing of the Vgf(24−39) peptide occurs at multiple sites to afford the following major products: Vgf-(30−39), Vfg(24−35), Vfg(24−34), and Vgf(24−33) (Figure 5).

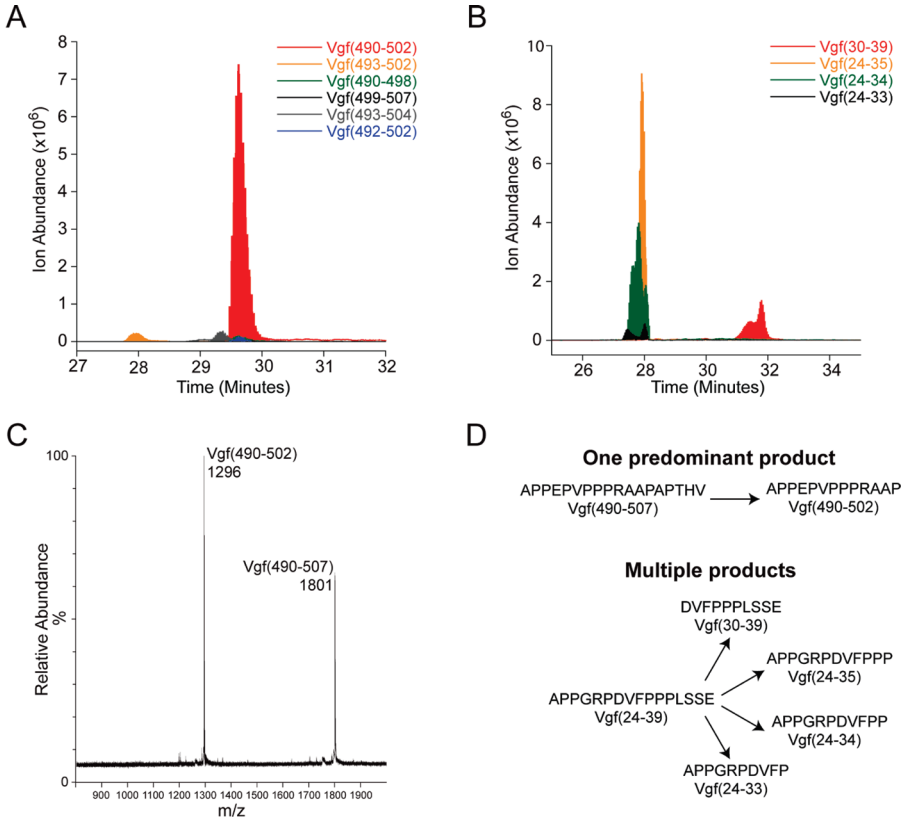

FIGURE 5: Prep cleavage of PRPs containing multiple prolines. (A) Cleavage of Vgf(490−507) by Prep occurs preferentially at a single position to provide Vgf(490−502) as the major product in the LC−MS trace. (B) PRP Vgf(24−39) is cleaved to similar extents at four prolines (positions 30 and 33−35). (C) A MALDI-MS spectrum of Vgf(490−507) supports the LC−MS data that show cleavage occurs preferentially at the proline at position 502 to give the product Vgf(490−502). (D) Cleavage pathways that generate the product distributions seen for Vgf(490−507) and Vgf(24−39).

By contrast, we find a single predominant cleavage product of the Vgf(409−507) peptide, Vgf(490−502), the endogenous product, indicating an increased rate of cleavage at this site at proline 502.

The studies revealed that certain peptides containing multiple proline residues are processed by Prep at a single site, while other peptides, with seemingly similar sequence motifs, are digested at multiple proline sites (Figures 4 and 5). For example, Prep cleaves the peptide Vgf(490−507) predominantly at the Pro13−Ala14 bond (Figure 5), even though there are eight potential Prep cleavage sites in this peptide, one after each proline. On the other hand, Prep cleaves another VGF peptide, Vgf(24−39), at multiple sites throughout the peptide, including the PPP repeat, which was suggested to be refractory to cleavage by any peptidase (*46*). Obviously, peptide structure could play a large role in regulating the cleavage specificity of the enzyme, but CD analysis revealed no substantial secondary structure in these peptides that could account for the observed differences in Prep specificity between the different sites (Supporting Information).

DISCUSSION

Here we utilized an unbiased peptidomics approach to identify the endogenous substrates of the peptidase Prep in the mouse CNS (spinal cord, brain, and hypothalamus). Earlier work aimed at identifying Prep substrates relied on radioimmunoassays and immunohistochemistry to measure changes in specific peptide levels as a function of Prep activity (*47*, *48*). For example, levels of substance P, α-melanocyte-stimulating hormone, thyrotrophin-releasing hormone, and arginine vasopressin are all elevated upon Prep inhibition in several discrete regions of the rat brain, as measured by immunohistochemical methods (*16*, *17*). Mass spectrometry-based peptidomics methods improve on these immunological methods because they are not restricted to known peptides, do not require associated antibodies, and are not subject to the cross-reactivity encountered by some antibodies (*49*).

In our studies, we used S17092 (*17*, *30*), which we confirmed as a selective Prep inhibitor (Figure 2A,B and the Supporting Information), to block Prep activity in the CNS. Comparison of the tissue peptidomes from S17092-treated mice to those of animals treated with vehicle revealed a number of peptide substrates for the enzyme, including the known substrate substance P (*14*, *17*). Surprisingly, there was no substrate overlap with a prior peptidomics study aimed at identifying Prep substrates in the CNS of rats. This could result from methodological differences such as inhibitor, model organism, duration of inhibition, or quantitation strategy. In total, we found changes in 23 distinct peptides, with levels of 15 peptides elevated in the S17092-treated samples (substrates) and levels of eight peptides elevated in the vehicle sample (products) (Table 1).

An overview of these peptides revealed that nine peptides (~40%) contain post-translational modifications (PTMs) and eight of these peptides (~35%) are protein fragments derived from regions of proteins known as PRDs. Three of the product peptides in the vehicle sample are shorter fragments of substrates found in the S17092-treated samples. For example, we detect the preproenkephalin peptide, Penk(123−133), in the vehicle-treated sample, while we see the level of corresponding Prep substrate,

Penk(114−133), elevated in the S17092-treated samples. We refer to these combinations where we are able to detect a substrate and its corresponding product as a "substrate−product pair". This provides us with the best evidence that a peptide is an endogenous substrate.

Prep substrates also included bioactive peptides, such as substance P. More generally, the measurement of changes in substance P levels upon Prep inhibition validates our methodology by demonstrating our ability to detect known Prep substrates. Furthermore, novel interactions between Prep and bioactive peptides were also detected. Specifically, the novel Prep substrate Penk(114−133), a fragment of the proenkephalin gene, has recently been shown to stimulate glutamate release when introduced into the brains of rodents (*50*). The determination of biological connections between Prep and bioactive peptides, such as Penk(114−133), is valuable because they highlight potential links between Prep and cellular and physiological functions, such as glutamate release in vivo.

In addition, the thymosin β4 peptides, Tmsb4(8−22) and Tmsb4(8−25), are precursors of the bioactive peptide Ac-SDKP, which is produced by Prep cleavage of thymosin β4 (*51*, *52*). The Ac-SDKP peptide has been implicated in a number of biological processes, including fibrosis, proliferation, and angiogenesis (*53*−*55*). While thymosin β4 is expressed in the brain, the Ac-SDKP peptide has mostly been studied in the periphery, specifically the cardiovascular system. Thus, the finding of thymosin β4 as a Prep substrate in the nervous system suggests that the Ac-SDKP peptide, and the thymosin β4-Prep-Ac-SDKP pathway in general, should also be studied for functions in the nervous system. This pathway could indicate new roles for Prep in the nervous system.

Next, we wanted to confirm that some of the S17092-elevated peptides were Prep substrates. We specifically targeted peptides that did not fit the typical mold of Prep substrates, which are usually short (< 15 residues) with a single proline (*12*, *14*, *16*, *56*), because we reasoned that looking at qualitatively different substrates provided the best opportunity to learn something new about the enzyme. Enzyme kinetics with recombinant Prep confirmed that CGRP(20−37) is a Prep substrate (Figure 3B,C). In an elegant series of studies, Gorrão and colleagues designed fluorescence resonance energy transfer (FRET) Prep substrates to study factors such as length dependence and subsite specificity of Prep (*41*). An exact comparison of results to this work is difficult because of differences in reaction conditions; however, it is clear that CGRP(20−27) is at least 2 orders of magnitude slower that a 17-residue peptide used by Gorrão and co-workers.

As mentioned, in vitro results are sometimes poor predictors of in vivo substrates, but this comparison does suggest that CGRP-(20−37) is probably not a preferred physiological substrate of Prep. Our in vivo data support this as well, since many of the better substrates return to baseline levels after 4 h, but the level of CGRP(20−37) is still elevated (Figure 2D). This suggests that the Prep is cleaving better substrates faster than it is cleaving CGRP(20−37) in vivo. Additionally, such poor substrates can sometimes also act as competitive inhibitors, which we demonstrated with CGRP(1−37). While it is possible that CGRP-(20−37) is also acting as an inhibitor, it is probably not occurring in vivo since CGRP(20−37) levels are up at 4 h while many of the preferred substrates (e.g., substance P) return to baseline levels, indicating a return of Prep activity.

Moreover, these FRET studies (*41*), as well as others (*57*), have demonstrated that longer peptides are poorer Prep substrates. For example, the aforementioned 17-residue FRET peptide was the worst substrate in a series of peptides ranging from 7 to 17 amino acids. We found similar results when comparing CGRP-(1−37) and dsCGRP(1−37), a di-serine mutant lacking the loop region found at the N-terminus of CGRP(1−37), to CGRP-(20−37), even though all these peptides contain the exact same 18-amino acid cleavage site. These kinetics experiments confirmed the preference of Prep for shorter substrates and demonstrated that Prep selectivity might allow the enzyme to control CGRP(20−37) without disturbing full-length CGRP(1−37) (Figure 3C), even though CGRP(20−37) is likely not a preferred endogenous Prep substrate.

Furthermore, experiments with a Prep mutant, PrepD35A-K196A, support the importance of interdomain interactions in providing access to the Prep active site (*11*, *40*, *43*), which is partly responsible for the length dependence seen with Prep (Figure 3C). Since the structures of these peptides are predominantly random coil (Supporting Information), and the mutant still shows a preference for shorter peptides, these results also suggest the additional possibility that longer peptides are interacting with the enzyme at an undefined exosite. Moreover, since CGRP(1−37) is a poor Prep substrate that still binds to the enzyme, we tested this peptide as a Prep inhibitor and showed that it could inhibit the cleavage of substance P with an IC_{50} of 2 μM. This provides a mechanism for explaining the previous observation that CGRP can enhance substance P activity (*44*, *45*) (Figure 3D). Without estimating intracellular concentrations of CGRP, it is impossible to assess whether this process is physiologically relevant, but this might provide an explanation for in vitro experiments with exogenously added CGRP (*45*). More generally, this experiment highlights the potential interplay between peptides and peptidases in the complex milieu of the cellular environment, providing another factor to consider when studying the mechanism of action of certain bioactive peptides.

One of the most striking contrasts between our results and the previous peptidomics analysis was the number of Prep-regulated peptides we identified that contain more than one proline. More specifically, 11 of 15 (~70%) of the substrates we identified had at least two prolines in the sequence, and seven of 15 endogenous substrates had more than two prolines, many of them derived from the PRDs of their precursor proteins (Table 1). PRDs are found in a number of proteins, including many scaffolding proteins, and mediate protein−protein interactions with SH3 proteins to assemble functional protein complexes (*58*−*60*). For example, the PRD of dynamin participates in protein−protein interactions between microtubules, Grb2, amphiphysin, and dynamin (i.e., dynamin−dynamin interactions) (*58*, *59*). Within a PRD, there are usually shorter sequences that mediate protein−protein interactions, including the consensus SH3 binding motif, XPXXP (*61*). Interestingly, we find an XPXXP motif in a number of the Prep-regulated peptides, including Vgf(490−507), Dnm1-(207−216), and Syn(673−682), which raises the possibility that these peptides might influence protein−protein interactions, through dominant-negative interactions.

We tested some of the substrates with multiple proline residues as substrates for Prep, including a pair of PRPs. One goal in these experiments was to gain evidence to support or refute an observation from our peptidomics data that suggests Prep shows a preference for individual prolines (Table 1). For example, despite having multiple proline residues, we detect only a single product for Vgf(490−507) in our vehicle-treated peptidomics data, Vgf(490−502), suggesting that this peptide is preferentially

cleaved at one of eight proline residues. By contrast, Penk-(123−133) is also a Prep product, but this peptide contains no prolines, indicating that both prolines are cleaved. We tested four peptides in these experiments as substrates for Prep: Penk-(114−133), Ac-Hsp12a(2−23), Vgf(24−39), and Vgf(490−507). On the basis of our in vivo results, we would predict that the Ac-Hsp12a(2−23), which contains two prolines, and Vgf(490−507), a PRP, would only preferentially be cleaved at a single site. Our in vitro experiments corroborated these predictions since Prep cleavage occurred predominantly at a single proline residue for both these peptides. By contrast, we found that the other two peptides, Penk(114−133) and Vgf(24−39), were processed to similar degrees at multiple sites to generate multiple fragments. Therefore, Prep can show a preference between proline residues in certain peptides, supporting the hypothesis developed from our peptidomics profiling data.

A cursory look at the peptide sequences that were preferentially cleaved at a single site to those peptides that were cleaved at multiple sites did not reveal any sequence elements that might provide a clue about the underlying molecular basis of this selectivity. For example, the two Vgf substrates, Vgf(24−39) and Vgf(490−507), both contain a PPP site, but the Vgf(24−39) peptide is cut at this site while the Vgf(490−507) peptide seems to be refractory to cleavage at this site. It is known that Prep can show some specificity based on charge near the cut site, preferring positively charged peptides at neutral pH (*56*). This specificity might provide an explanation for some of these differences, but we do not have enough substrates to identify such a pattern in our data. Furthermore, CD measurements indicated that most of the peptides are predominantly random coil in solution, so structural differences between the peptides cannot contribute strongly to these differences.

In conclusion, our peptidomics results have provided new insights into the biochemistry and biology of Prep in the nervous system. Prep-regulated peptides included known substrates such as substance P and thymosin β4, which validates our profiling results, as well as novel substrates, including PRPs. Biochemical experiments tested and confirmed a subset of S17092-elevated peptides as substrates of Prep. These experiments also provided insights into the biochemistry of the enzyme, revealing an unappreciated specificity that enables Prep to preferentially cleave at a single proline in peptides that contain multiple prolines. In addition to these biochemical insights, the discovery of bioactive peptides, or bioactive peptide precursors, regulated by Prep facilitates the development of new hypotheses about the physiological function of Prep. For example, elevated levels of thymosin β4 precursor protein indicate that Prep is controlling the production of the Ac-SDKP peptide in the nervous system, which would link Prep to the regulation of diverse physiological processes such as angiogenesis and proliferation in the CNS. More generally, these results highlight the value of peptidomics approaches in obtaining biochemical and biological insights into the functions of mammalian peptidases.

ACKNOWLEDGMENT

We thank the other members of our lab for reading the manuscript and for helpful discussions.

SUPPORTING INFORMATION AVAILABLE

ABPP gels with prolyl peptidases and S17092, Prep activity assay showing heat inactivation, graph with fold changes of peptides after inhibition for 1 and 4 h, graph of CGRP(1−37) levels after inhibition for 1 h, kinetic plots of CGRP analogues with wild-type and mutant Prep, table with kinetic parameters of CGRP analogues with wild-type and mutant Prep with k_{cat}/K_m calculated as a second-order rate constant, MALDI-MS spectrum of the reaction of unacetylated Hsp12a(2−23) with Prep, circular dichroism spectra used in in vitro studies with Prep, and a table showing the percent α-helicity of CGRP analogues. This material is available free of charge via the Internet at http://pubs.acs.org.

REFERENCES

1. Walter, R., Shlank, H., Glass, J. D., Schwartz, I. L., and Kerenyi, T. D. (1971) Leucylglycinamide released from oxytocin by human uterine enzyme. *Science 173*, 827–829.
2. Garcia-Horsman, J. A., Mannisto, P. T., and Venalainen, J. I. (2007) On the role of prolyl oligopeptidase in health and disease. *Neuropeptides 41*, 1–24.
3. Rosenblum, J. S., and Kozarich, J. W. (2003) Prolyl peptidases: A serine protease subfamily with high potential for drug discovery. *Curr. Opin. Chem. Biol. 7*, 496–504.
4. Weber, A. E. (2004) Dipeptidyl peptidase IV inhibitors for the treatment of diabetes. *J. Med. Chem. 47*, 4135–4141.
5. Szeltner, Z., Alshafee, I., Juhasz, T., Parvari, R., and Polgar, L. (2005) The PREPL A protein, a new member of the prolyl oligopeptidase family, lacking catalytic activity. *Cell. Mol. Life Sci. 62*, 2376–2381.
6. Jaeken, J., Martens, K., Francois, I., Eyskens, F., Lecointre, C., Derua, R., Meulemans, S., Slootstra, J. W., Waelkens, E., de Zegher, F., Creemers, J. W., and Matthijs, G. (2006) Deletion of PREPL, a gene encoding a putative serine oligopeptidase, in patients with hypotonia-cystinuria syndrome. *Am. J. Hum. Genet. 78*, 38–51.
7. Martens, K., Derua, R., Meulemans, S., Waelkens, E., Jaeken, J., Matthijs, G., and Creemers, J. W. (2006) PREPL: A putative novel oligopeptidase propelled into the limelight. *Biol. Chem. 387*, 879–883.
8. Chabrol, B., Martens, K., Meulemans, S., Cano, A., Jaeken, J., Matthijs, G., and Creemers, J. W. (2008) Deletion of C2orf34, PREPL and SLC3A1 causes atypical hypotonia-cystinuria syndrome. *J. Med. Genet. 45*, 314–318.
9. Leiting, B., Pryor, K. D., Wu, J. K., Marsilio, F., Patel, R. A., Craik, C. S., Ellman, J. A., Cummings, R. T., and Thornberry, N. A. (2003) Catalytic properties and inhibition of proline-specific dipeptidyl peptidases II, IV and VII. *Biochem. J. 371*, 525–532.
10. Polgar, L. (1991) pH-dependent mechanism in the catalysis of prolyl endopeptidase from pig muscle. *Eur. J. Biochem. 197*, 441–447.
11. Fulop, V., Bocskei, Z., and Polgar, L. (1998) Prolyl oligopeptidase: An unusual β-propeller domain regulates proteolysis. *Cell 94*, 161–170.
12. Moriyama, A., Nakanishi, M., and Sasaki, M. (1988) Porcine muscle prolyl endopeptidase and its endogenous substrates. *J. Biochem. 104*, 112–117.
13. Wilk, S. (1983) Prolyl endopeptidase. *Life Sci. 33*, 2149–2157.
14. Toide, K., Okamiya, K., Iwamoto, Y., and Kato, T. (1995) Effect of a novel prolyl endopeptidase inhibitor, JTP-4819, on prolyl endopeptidase activity and substance P- and arginine-vasopressin-like immunoreactivity in the brains of aged rats. *J. Neurochem. 65*, 234–240.
15. Shinoda, M., Okamiya, K., and Toide, K. (1995) Effect of a novel prolyl endopeptidase inhibitor, JTP-4819, on thyrotropin-releasing hormone-like immunoreactivity in the cerebral cortex and hippocampus of aged rats. *Jpn. J. Pharmacol. 69*, 273–276.
16. Bellemere, G., Vaudry, H., Morain, P., and Jegou, S. (2005) Effect of prolyl endopeptidase inhibition on arginine-vasopressin and thyrotrophin-releasing hormone catabolism in the rat brain. *J. Neuroendocrinol. 17*, 306–313.
17. Bellemere, G., Morain, P., Vaudry, H., and Jegou, S. (2003) Effect of S 17092, a novel prolyl endopeptidase inhibitor, on substance P and α-melanocyte-stimulating hormone breakdown in the rat brain. *J. Neurochem. 84*, 919–929.
18. Toide, K., Iwamoto, Y., Fujiwara, T., and Abe, H. (1995) JTP-4819: A novel prolyl endopeptidase inhibitor with potential as a cognitive enhancer. *J. Pharmacol. Exp. Ther. 274*, 1370–1378.
19. Jalkanen, A. J., Puttonen, K. A., Venalainen, J. I., Sinerva, V., Mannila, A., Ruotsalainen, S., Jarho, E. M., Wallen, E. A., and Mannisto, P. T. (2007) Beneficial effect of prolyl oligopeptidase inhibition on spatial memory in young but not in old scopolamine-treated rats. *Basic Clin. Pharmacol. Toxicol. 100*, 132–138.

20. Morain, P., Lestage, P., De Nanteuil, G., Jochemsen, R., Robin, J. L., Guez, D., and Boyer, P. A. (2002) S 17092: A prolyl endopeptidase inhibitor as a potential therapeutic drug for memory impairment. Preclinical and clinical studies. *CNS Drug Rev. 8*, 31–52.
21. Williams, R. S., Cheng, L., Mudge, A. W., and Harwood, A. J. (2002) A common mechanism of action for three mood-stabilizing drugs. *Nature 417*, 292–295.
22. Tenorio-Laranga, J., Valero, M. L., Mannisto, P. T., Sanchez del Pino, M., and Garcia-Horsman, J. A. (2009) Combination of snap freezing, differential pH two-dimensional reverse-phase high-performance liquid chromatography, and iTRAQ technology for the peptidomic analysis of the effect of prolyl oligopeptidase inhibition in the rat brain. *Anal. Biochem. 393*, 80–87.
23. Svensson, M., Skold, K., Svenningsson, P., and Andren, P. E. (2003) Peptidomics-based discovery of novel neuropeptides. *J. Proteome Res. 2*, 213–219.
24. Brockmann, A., Annangudi, S. P., Richmond, T. A., Ament, S. A., Xie, F., Southey, B. R., Rodriguez-Zas, S. R., Robinson, G. E., and Sweedler, J. V. (2009) Quantitative peptidomics reveal brain peptide signatures of behavior. *Proc. Natl. Acad. Sci. U.S.A. 106*, 2383–2388.
25. Zhang, X., Che, F. Y., Berezniuk, I., Sonmez, K., Toll, L., and Fricker, L. D. (2008) Peptidomics of Cpe(fat/fat) mouse brain regions: Implications for neuropeptide processing. *J. Neurochem. 107*, 1596–1613.
26. Pan, H., Nanno, D., Che, F. Y., Zhu, X., Salton, S. R., Steiner, D. F., Fricker, L. D., and Devi, L. A. (2005) Neuropeptide processing profile in mice lacking prohormone convertase-1. *Biochemistry 44*, 4939–4948.
27. Che, F. Y., Lim, J., Pan, H., Biswas, R., and Fricker, L. D. (2005) Quantitative neuropeptidomics of microwave-irradiated mouse brain and pituitary. *Mol. Cell. Proteomics 4*, 1391–1405.
28. Tagore, D. M., Nolte, W. M., Neveu, J. M., Rangel, R., Guzman-Rojas, L., Pasqualini, R., Arap, W., Lane, W. S., and Saghatelian, A. (2009) Peptidase substrates via global peptide profiling. *Nat. Chem. Biol. 5*, 23–25.
29. Williamson, M. P. (1994) The structure and function of proline-rich regions in proteins. *Biochem. J. 297* (Part 2), 249–260.
30. Portevin, B., Benoist, A., Remond, G., Herve, Y., Vincent, M., Lepagnol, J., and De Nanteuil, G. (1996) New prolyl endopeptidase inhibitors: In vitro and in vivo activities of azabicyclo[2.2.2]octane, azabicyclo[2.2.1]heptane, and perhydroindole derivatives. *J. Med. Chem. 39*, 2379–2391.
31. Leung, D., Hardouin, C., Boger, D. L., and Cravatt, B. F. (2003) Discovering potent and selective reversible inhibitors of enzymes in complex proteomes. *Nat. Biotechnol. 21*, 687–691.
32. Patricelli, M. P., Giang, D. K., Stamp, L. M., and Burbaum, J. J. (2001) Direct visualization of serine hydrolase activities in complex proteomes using fluorescent active site-directed probes. *Proteomics 1*, 1067–1071.
33. Barelli, H., Petit, A., Hirsch, E., Wilk, S., De Nanteuil, G., Morain, P., and Checler, F. (1999) S 17092-1, a highly potent, specific and cell permeant inhibitor of human proline endopeptidase. *Biochem. Biophys. Res. Commun. 257*, 657–661.
34. Smith, C. A., Want, E. J., O'Maille, G., Abagyan, R., and Siuzdak, G. (2006) XCMS: Processing mass spectrometry data for metabolite profiling using nonlinear peak alignment, matching, and identification. *Anal. Chem. 78*, 779–787.
35. Eng, J. K., McCormack, A. L., and Yates, J. R., III (1994) An approach to correlate tandem mass spectral data of peptides with amino acid sequences in a protein database. *J. Am. Soc. Mass Spectrom. 5*, 976–989.
36. Yoshimoto, T., Ogita, K., Walter, R., Koida, M., and Tsuru, D. (1979) Post-proline cleaving enzyme. Synthesis of a new fluorogenic substrate and distribution of the endopeptidase in rat tissues and body fluids of man. *Biochim. Biophys. Acta 569*, 184–192.
37. Parkin, M. C., Wei, H., O'Callaghan, J. P., and Kennedy, R. T. (2005) Sample-dependent effects on the neuropeptidome detected in rat brain tissue preparations by capillary liquid chromatography with tandem mass spectrometry. *Anal. Chem. 77*, 6331–6338.
38. Wikoff, W. R., Anfora, A. T., Liu, J., Schultz, P. G., Lesley, S. A., Peters, E. C., and Siuzdak, G. (2009) Metabolomics analysis reveals large effects of gut microflora on mammalian blood metabolites. *Proc. Natl. Acad. Sci. U.S.A. 106*, 3698–3703.
39. Nordstrom, A., O'Maille, G., Qin, C., and Siuzdak, G. (2006) Nonlinear data alignment for UPLC-MS and HPLC-MS based metabolomics: Quantitative analysis of endogenous and exogenous metabolites in human serum. *Anal. Chem. 78*, 3289–3295.
40. Shan, L., Mathews, I. I., and Khosla, C. (2005) Structural and mechanistic analysis of two prolyl endopeptidases: Role of interdomain dynamics in catalysis and specificity. *Proc. Natl. Acad. Sci. U.S.A. 102*, 3599–3604.
41. Gorrao, S. S., Hemerly, J. P., Lima, A. R., Melo, R. L., Szeltner, Z., Polgar, L., Juliano, M. A., and Juliano, L. (2007) Fluorescence resonance energy transfer (FRET) peptides and cycloretro-inverso peptides derived from bradykinin as substrates and inhibitors of prolyl oligopeptidase. *Peptides 28*, 2146–2154.
42. Camargo, A. C., Caldo, H., and Reis, M. L. (1979) Susceptibility of a peptide derived from bradykinin to hydrolysis by brain endo-oligopeptidases and pancreatic proteinases. *J. Biol. Chem. 254*, 5304–5307.
43. Fuxreiter, M., Magyar, C., Juhasz, T., Szeltner, Z., Polgar, L., and Simon, I. (2005) Flexibility of prolyl oligopeptidase: Molecular dynamics and molecular framework analysis of the potential substrate pathways. *Proteins 60*, 504–512.
44. Mao, J., Coghill, R. C., Kellstein, D. E., Frenk, H., and Mayer, D. J. (1992) Calcitonin gene-related peptide enhances substance P-induced behaviors via metabolic inhibition: In vivo evidence for a new mechanism of neuromodulation. *Brain Res. 574*, 157–163.
45. Le Greves, P., Nyberg, F., Terenius, L., and Hokfelt, T. (1985) Calcitonin gene-related peptide is a potent inhibitor of substance P degradation. *Eur. J. Pharmacol. 115*, 309–311.
46. Vanhoof, G., Goossens, F., De Meester, I., Hendriks, D., and Scharpe, S. (1995) Proline motifs in peptides and their biological processing. *FASEB J. 9*, 736–744.
47. Rehfeld, J. F. (1998) How to measure cholecystokinin in tissue, plasma and cerebrospinal fluid. *Regul. Pept. 78*, 31–39.
48. Hokfelt, T., Broberger, C., Xu, Z. Q., Sergeyev, V., Ubink, R., and Diez, M. (2000) Neuropeptides: An overview. *Neuropharmacology 39*, 1337–1356.
49. Jankowski, V., Vanholder, R., van der Giet, M., Tolle, M., Karadogan, S., Gobom, J., Furkert, J., Oksche, A., Krause, E., Tran, T. N., Tepel, M., Schuchardt, M., Schluter, H., Wiedon, A., Beyermann, M., Bader, M., Todiras, M., Zidek, W., and Jankowski, J. (2007) Mass-spectrometric identification of a novel angiotensin peptide in human plasma. *Arterioscler. Thromb. Vasc. Biol. 27*, 297–302.
50. Bernay, B., Gaillard, M. C., Guryca, V., Emadali, A., Kuhn, L., Bertrand, A., Detraz, I., Carcenac, C., Savasta, M., Brouillet, E., Garin, J., and Elalouf, J. M. (2009) Discovering new bioactive neuropeptides in the striatum secretome using in vivo microdialysis and versatile proteomics. *Mol. Cell. Proteomics 8*, 946–958.
51. Cavasin, M. A., Rhaleb, N. E., Yang, X. P., and Carretero, O. A. (2004) Prolyl oligopeptidase is involved in release of the antifibrotic peptide Ac-SDKP. *Hypertension 43*, 1140–1145.
52. Cavasin, M. A., Liao, T. D., Yang, X. P., Yang, J. J., and Carretero, O. A. (2007) Decreased endogenous levels of Ac-SDKP promote organ fibrosis. *Hypertension 50*, 130–136.
53. Rossdeutsch, A., Smart, N., and Riley, P. R. (2008) Thymosin β4 and Ac-SDKP: Tools to mend a broken heart. *J. Mol. Med. 86*, 29–35.
54. Sharma, U., Rhaleb, N. E., Pokharel, S., Harding, P., Rasoul, S., Peng, H., and Carretero, O. A. (2008) Novel anti-inflammatory mechanisms of N-Acetyl-Ser-Asp-Lys-Pro in hypertension-induced target organ damage. *Am. J. Physiol. 294*, H1226–H1232.
55. Huang, W. Q., Wang, B. H., and Wang, Q. R. (2006) Thymosin β4 and AcSDKP inhibit the proliferation of HL-60 cells and induce their differentiation and apoptosis. *Cell Biol. Int. 30*, 514–520.
56. Polgar, L. (1992) Unusual secondary specificity of prolyl oligopeptidase and the different reactivities of its two forms toward charged substrates. *Biochemistry 31*, 7729–7735.
57. Quinto, B. M., Juliano, M. A., Hirata, I., Carmona, A. K., Juliano, L., and Casarini, D. E. (2000) Characterization of a prolyl endopeptidase (kininase) from human urine using fluorogenic quenched substrates. *Int. J. Biochem. Cell Biol. 32*, 1161–1172.
58. Grabs, D., Slepnev, V. I., Songyang, Z., David, C., Lynch, M., Cantley, L. C., and De Camilli, P. (1997) The SH3 domain of amphiphysin binds the proline-rich domain of dynamin at a single site that defines a new SH3 binding consensus sequence. *J. Biol. Chem. 272*, 13419–13425.
59. Hinshaw, J. E., and Schmid, S. L. (1995) Dynamin self-assembles into rings suggesting a mechanism for coated vesicle budding. *Nature 374*, 190–192.
60. Macias, M. J., Wiesner, S., and Sudol, M. (2002) WW and SH3 domains, two different scaffolds to recognize proline-rich ligands. *FEBS Lett. 513*, 30–37.
61. Mongiovi, A. M., Romano, P. R., Panni, S., Mendoza, M., Wong, W. T., Musacchio, A., Cesareni, G., and Di Fiore, P. P. (1999) A novel peptide-SH3 interaction. *EMBO J. 18*, 5300–5309.